

A Truncated Form of SpoT, Including the ACT Domain, Inhibits the Production of Cyclic Lipopeptide Arthrofactin, and Is Associated with Moderate Elevation of Guanosine 3',5'-Bispyrophosphate Level in *Pseudomonas* sp. MIS38

Kenji WASHIO,^{1,†} Siew Ping LIM,² Niran ROONGSAWANG,³ and Masaaki MORIKAWA¹

¹Division of Biosphere Science, Graduate School of Environmental Science, Hokkaido University, Sapporo 060-0810, Japan

²School of Science, Monash University Sunway Campus Sdn Bhd, Jalan Lagoon Selatan, 46150 Bandar Sunway, Selangor, Malaysia

³BIOTEC Central Research Unit, Thai National Center for Genetic Engineering and Biotechnology, Pathumthani 12120, Thailand

Received January 17, 2011; Accepted July 20, 2011; Online Publication, October 7, 2011

[doi:10.1271/bbb.110042]

Arthrofactin is a biosurfactant produced by *Pseudomonas* sp. MIS38. We have reported that transposon insertion into *spoT* (*spoT::Tn5*) causes moderate accumulation of guanosine 3',5'-bispyrophosphate (ppGpp) and abrogates arthrofactin production. To analyze the linkage of SpoT function and ablation of arthrofactin production, we examined the *spoT::Tn5* mutation. The results showed that *spoT::Tn5* is not a null mutation, but encodes separate segments of SpoT. Deletion of the 3' region of *spoT* increased the level of arthrofactin production, suggesting that the C-terminal region of SpoT plays a suppressive role. We evaluated the expression of a distinct segment of SpoT. Forced expression of the C-terminal region that contains the ACT domain resulted in the accumulation of ppGpp and abrogated arthrofactin production. Expression of the C-terminal segment also reduced MIS38 swarming and resulted in extensive biofilm formation, which constitutes the phenocopy of the *spoT::Tn5* mutant.

Key words: ACT domain; arthrofactin; nonribosomal peptide synthetase; (p)ppGpp; *spoT*

Nonribosomal peptide synthetase (NRPS) is a class of multimodular enzymes that synthesize various bioactive products in bacteria and fungi.¹⁾ *Pseudomonas* sp. MIS38 produces the cyclic lipopeptide arthrofactin, which contains a head group of 11 amino acids linked to a β -hydroxydecanoyl tail.²⁾ We have examined the biochemical properties of arthrofactin, which is more amphiphilic than other surfactants and one of the most effective biosurfactants examined to date.³⁾ Extensive analysis identified a gene cluster responsible for the biosynthesis of arthrofactin,⁴⁾ and confirmed that arthrofactin synthesis is conducted by a mega complex of three NRPS subunits, ArfA, ArfB, and ArfC.⁵⁾ A failure of arthrofactin production impairs swarming and biofilm formation, suggesting that arthrofactin plays a crucial role in the social behavior of MIS38.⁴⁾

To analyze the mechanisms controlling arthrofactin production, we employed transposon 5' (Tn5)-based

mutagenesis, and obtained a series of arthrofactin-deficient mutants.⁶⁾ In these mutants, Tn5 insertion into the *spoT* locus (*spoT::Tn5*) reduced arthrofactin production. *spoT* encodes a bifunctional enzyme, SpoT, that degrades guanosine 3',5'-bispyrophosphate (ppGpp) and also synthesizes guanosine 3'-diphosphate 5'-triphosphate (pppGpp).⁷⁾ Since pppGpp is hydrolyzed by ubiquitous phosphatases in the cell, and is promptly converted to ppGpp, the combination of pppGpp and ppGpp is collectively called (p)ppGpp. (p)ppGpp regulates the stringent response that downregulates ribosome production and increases the transcription of the genes involved in amino acid biosynthesis.⁸⁾ It is also accepted that (p)ppGpp acts on particular secondary metabolisms for the ecological fitness of bacteria.⁹⁾

In general, Gram-negative bacteria have two distinct enzymes, RelA and SpoT, which control (p)ppGpp levels.¹⁰⁾ RelA is a primary pppGpp synthetase in amino acid limitation. SpoT probably degrades ppGpp under non-stressful conditions, and weakly synthesizes pppGpp under nutrient starvation. Because the major role of SpoT lies in the breakdown of ppGpp, (p)ppGpp levels gradually increase in the absence of SpoT due to the remaining activity of RelA, and this results in severe growth arrest¹¹⁾ or causes extra nutrient demands.¹²⁾ Thus *spoT* is essential for most Gram-negative bacteria, but the specific roles of *spoT* in individual bacteria are largely unknown.

We have generated the *spoT::Tn5* mutation in the *relA*⁺ background of MIS38, and we found that the increase in the ppGpp level was moderate in our mutant.⁶⁾ This suggests that a portion of *spoT* is functional. RelA, SpoT, and homologous (RSH) proteins are composed of multiple functional domains. SpoT contains the His-Asp (HD) and RSD domains in the N-terminal half, which is responsible for the hydrolysis and synthesis of (p)ppGpp. The TGS and ACT domains present in the C-terminal half have regulatory functions. Previous analyses indicate that distinct expression of the functional domains derived from RelA and from SpoT exert various effects on (p)ppGpp metabolism.¹³⁾ Given

[†] To whom correspondence should be addressed. Fax: +81-11-706-2281; E-mail: washi@ees.hokudai.ac.jp

Table 1. Oligonucleotide Primers Used in the Experiments

Oligonucleotide primers for the chromosome walking PCR of MIS38 DNA		
Gene	Forward primer	Reverse primer
<i>salA</i> -like (<i>arfG</i>)	<i>salA</i> _f, 5'-AGTGCCCGGTGCCGCTGCAC-3'	<i>salA</i> _r, 5'-CTGCAGATCGGGCACCATCA-3'
Oligonucleotide primers for the RT-PCR analysis		
Gene	Forward primer	Reverse primer
<i>arfB</i>	<i>arfB</i> _f, 5'-GGCAAACCTCGACCGCAAGGC-3'	<i>arfB</i> _r, 5'-GGCGTAGCCTGCCAAGGTCG-3'
<i>arfF</i>	<i>arfF</i> _f, 5'-TCGTGCAACACCTGCTGCAA-3'	<i>arfF</i> _r, 5'-GTCGCTCCAGCCGCAACATC-3'
<i>arfG</i>	<i>arfG</i> _f, 5'-GCGGATGCTGCATGACCTGA-3'	<i>arfG</i> _r, 5'-TCCTTGCGCCGGGTGAGGTG-3'
<i>spoT</i>	<i>spoT</i> _f, 5'-TCGGCGAAGGCGAACAGCTG-3'	<i>spoT</i> _r, 5'-TTCCAGCTCGACGCGCAGCT-3'
<i>spoT_{Nter}</i>	<i>spoT_{Nter}</i> _f, 5'-CGTCAAGGCGATGCTCACCG-3' (MIS38)	<i>spoT_{Nter}</i> _r, 5'-ATAAAGCTTGCTCAATCAATCACC-3' (Tn5)
<i>spoT_{Cter}</i>	<i>spoT_{Cter}</i> _f, 5'-GATCAAGAGACAGGCCCGGA-3' (Tn5)	<i>spoT_{Cter}</i> _r, 5'-TTCCAGCTCGACGCGCAGCT-3' (MIS38)
<i>16S rRNA</i>	<i>16S</i> _f, 5'-ACGGGTGAGTAATGCCTAGG-3'	<i>16S</i> _r, 5'-CAGGCTTTCGCCCATTTGCC-3'
Oligonucleotide primers for the gene manipulation of <i>spoT</i> in <i>P. sp.</i> MIS38		
Gene	Forward primer	Reverse primer
<i>spoT</i> -null 5' region	<i>null5</i> _f, 5'-GCGCTCTAGATTGGTGTGCTGACGCGCT-3'	<i>null5</i> _r, 5'-CGAGGTCTTCGAATTCGATACG-3'
<i>spoT</i> -null 3' region	<i>null3</i> _f, 5'-CCGGCGAATCAACGTCGAG-3'	<i>null3</i> _r, 5'-ATCACCTGCAGCCGTCCTTC-3'
<i>spoT-delC</i> 5' region	<i>del5</i> _f, 5'-GGTCTAGAGCGCCCGGGCAACCGCAAG-3'	<i>del5</i> _r, 5'-ATAAAGCTTGCTCAATCAATCACC-3'
<i>spoT-delC</i> 3' region	<i>del3</i> _f, 5'-CTAAGCTTACCTAACAAAGGAGTCATAC-3'	<i>del3</i> _r, 5'-CCGTCGACTTCCAGGCGCCGGAC-3'
Oligonucleotide primers for the overexpression analysis with pME6032		
Gene	Forward primer	Reverse primer
<i>arfF</i>	<i>arfF</i> _exf, 5'-ACGAGCTCATGAATCTGACCGGCAGCAT-3'	<i>arfF</i> _exr, 5'-CCCTCGAGTTATGCCCGCCATCCAGC-3'
<i>arfG</i>	<i>arfG</i> _exf, 5'-CAGAGCTCATGCTCGACGCAGGTCAGGA-3'	<i>arfG</i> _exr, 5'-CGGGTACCATCAAGCGGCTGGGGTGAG-3'
<i>spoT</i>	<i>spoT</i> _exf, 5'-GCGGGAGCTCAGCCTACGGCAGGAG-3'	<i>spoT</i> _exr, 5'-GGGGTACCTTAGGCACGCATGCGGGTGA-3'
<i>spoT_{Nter}</i>	<i>spoT_{Nter}</i> _exf, 5'-GCGGGAGCTCAGCCTACGGCAGGAG-3'	<i>spoT_{Nter}</i> _exr, 5'-ATAAAGCTTGCTCAATCAATCACC-3' (Tn5)
<i>spoT_{Cter}</i>	<i>spoT_{Cter}</i> _exf, 5'-GAGCTCCGCAAGCATCAGG-3' (Tn5)	<i>spoT_{Cter}</i> _exr, 5'-GGGGTACCTTAGGCACGCATGCGGGTGA-3'

this information, we assumed that the function of *spoT* might be modified due to the *spoT::Tn5* mutation.

The *spoT::Tn5* mutation also resulted in pleiotropic effects on the social behavior of MIS38, including a complete loss of swarming and prolonged biofilm formation.⁶⁾ These findings are partly consistent with the phenotypes caused by a failure of arthrfactin production.⁴⁾ This suggests that arthrfactin production is governed by the global function of SpoT. Here we examined the *spoT::Tn5* mutation of MIS38 in more detail.

Materials and Methods

Bacterial strains and growth conditions. *Pseudomonas* sp. MIS38 (NCBI taxonomy ID 91465)²⁾ and the mutant strains were grown in LB liquid medium at 30 °C with shaking at 150 rpm. For the swarming assay, 1 µL of the culture (OD₆₀₀ = 0.5) was placed at the center of a 0.7% LB agar plate and incubated at 30 °C for 12 h. The swarming area was determined by measuring the diameter of the swarming colony. Cloning vectors pBluescript II SK⁺ (Stratagene, La Jolla, CA) and pGEM-T EASY (Promega, Madison, WI) were used in *Escherichia coli* NovaBlue (Novagen, Madison, WI) for general cloning of the DNA fragments. Plasmid pME6032 was used as gene expression vector for MIS38 and the *spoT::Tn5* mutant strains.¹⁴⁾

General DNA manipulation. The nucleotide sequence of the *salA*-like gene was obtained from the genome information of the closest

relative of MIS38, *Pseudomonas fluorescence* Pfo-1 (accession no. CP000094), and a set of suitable PCR primers was constructed (Table 1). A DNA fragment containing *arfG* was successfully amplified by PCR using MIS38 genomic DNA. The PCR products were gel-purified using a QIAquick Gel Extraction Kit (Qiagen, Hilden, Germany) and cloned. Nucleotide sequences were determined by BigDye terminator cycle sequencing on an ABI Model 3130 DNA Sequencer (Perkin-Elmer Applied Biosystems, Wellesley, MA). Sequence data have been submitted to the public database under accession nos. AB107223 (*arfA/B/C* and *arfF*), AB286215 (the 3' region of the *arfA/B/C* operon), AB359232 (*arfG*), and AB262446 (*spoT*).

HPLC analysis of arthrfactin production. MIS38 and mutant strains were grown in LB medium at 30 °C for 2 d. Bacterial cells were removed by centrifugation twice at 10,000 × *g* for 15 min at 4 °C. The culture supernatants were acidified to pH 2.0 by the addition of 6 N HCl, and the hydrophobic fractions containing arthrfactin were precipitated at 4 °C. The precipitates were dissolved in 100% methanol. The final sample was diluted to 10% v/v methanol, and a portion (200 µL) was subjected to reverse-phase HPLC analysis as described previously (HP1100) (Hewlett Packard, Chicago, IL).⁴⁾ Arthrfactin production is presented as relative peak areas (%) as compared to that of the wild type. The data set represents the mean values ± standard errors for triplicate experiments.

Construction of gene expression vectors. Gene fragments spanning the entire coding region of *arfF*, *arfG*, and *spoT* were amplified by PCR using the specific primers pairs (Table 1). The amplified

fragments were recovered from agarose gel electrophoresis, digested with *Sac* I and *Kpn* I (underlined in Table 1) or blunt-ended, and cloned into the corresponding sites of pME6032. The resulting plasmids, pSpoT6032; *P_{tac}::spoT* (1–701 aa), pArfG6032; *P_{tac}::arfG* (1–274 aa), and pArfF6032; *P_{tac}::arfF* (1–264 aa), were introduced into the *spoT::Tn5* mutant by electroporation. The DNA fragments to be used to express the distinct segment of SpoT were amplified by PCR using the genomic DNA of the *spoT::Tn5* mutant and the specific primers pairs (Table 1), and were cloned into pME6032. The exogenous gene in pME6032 was inducible by the control of the *tac* promoter. Transformants were grown in LB medium supplemented with 12.5 µg/mL of tetracycline and 1 mM isopropyl-β-D-thiogalactopyranoside.

Reverse transcriptase (RT)-PCR analysis. Total RNA was extracted from bacterial cells using an RNeasy Mini Kit (Qiagen). cDNA was synthesized from 1 µg of DNase-treated RNA, as described previously,¹⁵ and subjected to PCR amplification using a set of primers specific for the target gene (Table 1) and Ex Taq DNA polymerase (Takara Bio, Shiga, Japan). PCR amplification was conducted as follows: 3 min at 94 °C, followed by 25 (*16S rRNA*), 30 (*arfB*, *arfF*, and *arfG*), or 35 (*spoT*, *spoT_{Nter}*, and *spoT_{Cter}*) cycles of 30 s at 94 °C, 30 s at 58 °C, and 30 s at 72 °C, and extension for 3 min at 72 °C. The PCR products were separated by 1.5% agarose gel electrophoresis in TBE (89 mM Tris-borate, 2 mM EDTA) and visualized by ethidium bromide staining. *16S rRNA* was used as internal control to normalize the amount of template.

Homologous recombination of *spoT* in MIS38. The gene fragments of interest from the MIS38 DNA were amplified by PCR (Table 1) and cloned into suicide vector pCVD442-Km, which was constructed by the insertion of a kanamycin resistance gene cassette at the *Sac* I site of pCVD442.¹⁶ The resulting plasmids were introduced into *E. coli* SM10 λ-pir. The pCVD442-Km plasmid was transferred into MIS38 by conjugation.⁶ After completion of conjugal transfer, bacterial cells were recovered in 10 mM MgSO₄ and spread onto a 1.5% LB agar plate containing 30 µg/mL of kanamycin and 10 µg/mL of chloramphenicol. Recombinant strains with resistance to kanamycin and chloramphenicol were selected and transferred to a 1.5% LB agar plate containing 6% w/v sucrose for counter-selection. Allelic changes of *spoT* were confirmed by PCR amplification.

Biofilm formation. Biofilm formation was examined as described previously.¹⁷ After standing cultivation at 20 °C in a 1.5-mL polypropylene tube (TC131615) (Nippon Genetics, Tokyo) containing 300 µL of LB medium, the biofilm surface was rinsed with distilled water and stained with 500 µL of 0.1% w/v crystal violet (CV) solution for 25 min. The CV solution was removed and the tube was washed twice with distilled water. The CV attached to the biofilm was dissolved in 400 µL of 95% v/v ethanol and quantified by measurement of the absorbance at 590 nm.

Scanning electron microscopy (SEM). Biofilms grown in a 1.5-mL polypropylene tube at 20 °C for 4 d were fixed with 2% v/v glutaraldehyde for 2 h and post-fixed with 2% OsO₄ in 0.1 M phosphate-buffered saline (pH 7.0) for 2 h. The fixed samples were dehydrated through a series of graded ethanol solutions, critical point dried, and then coated with gold-palladium under high vacuum. The samples were observed using a Model S-2400 scanning electron microscope (Hitachi, Tokyo).

ppGpp analysis. After cultivation in LB liquid medium at 30 °C for 2 d, nucleotides were extracted with formic acid.^{6,8} The nucleotide sample (200 µL) was separated by ion-pair reverse-phase HPLC with a Cosmosil 5C₁₈ AR II column (4.6 × 150 mm, Nacalai Tesque, Kyoto, Japan) at a flow rate of 1.0 mL/min. The mobile phase consisted of 125 mM potassium phosphate buffer (pH 6.0) containing 10 mM tetrabutyl ammonium dihydrogen phosphate and 6% v/v methanol.¹⁸ The eluted nucleotides were monitored by sample absorbance at 254 nm and identified by comparison of the elution time with authentic standards. The ppGpp standard was purchased from Trilink Biotechnologies (San Diego, CA).

Results

Transcriptional control of arthrofactin production

The bacterial relatives of MIS38, including *Pseudomonas fluorescens* PfO-1, *Pseudomonas fluorescens* Pf-5, and *Pseudomonas syringae* pv. *syringae* B301D, have similar NRPS gene clusters associated with the production of arthrofactin-like lipopeptides, in which the *syrF*- and *salA*-like genes for the LuxR-type transcription regulator are embedded (Fig. 1A).¹⁹ A study of B301D documented that SyrF can transactivate the target NRPS promoters responsible for the biosynthesis of two lipopeptides, syringomycin (*syr*) and syringopeptin (*syp*).¹⁹ SalA is an essential upstream regulator that positively controls the expression of the *syr* and *syp* synthetase genes and the *syrF* regulatory gene.²⁰

Our previous study indicated that loss of the *arfF* function (*arfF::Tn5*) reduces arthrofactin production.⁶ *arfF* is the evident homolog of *syrF* and locates just upstream of the arthrofactin synthetase operon (Fig. 1A). This suggests that the transcription control of arthrofactin production is similar to that of related bacteria. Even though SyrF-like and SalA-like proteins appear to regulate the production of arthrofactin-like lipopeptides coordinately, we did not find any *salA* homologs near the arthrofactin synthetase operon (accession no. AB286215).²¹ Hence we searched for a *salA*-like gene in MIS38, dubbed *arfG*, and found it at a distinct gene locus near a universal stress protein gene (AB359232). The predicted protein structure of ArfG (274 aa) shared sequence identity with LuxR family proteins from *P. fluorescens* PfO-1 (ABA73959, identity 74%), *P. fluorescens* Pf-5 (AAY91424, 62%), and with SalA from *P. syringae* pv. *syringae* B301D (AAK83335, 41%).

Although the role of this SalA-like protein in arthrofactin production is unclear, the expression patterns of *arfB*, *arfF*, and *arfG* were monitored in the *arfF::Tn5* and *spoT::Tn5* mutants (Fig. 1B). RT-PCR analysis indicated that the expression of *arfF* and of *arfB* declined in the *arfF::Tn5* mutant, while that of *arfG* did not change. The transcript levels of *spoT*, *arfG*, *arfF*, and *arfB* were uniformly downregulated in the *spoT::Tn5* mutant. These results suggest that ArfF is the direct regulator of *arfB* and that SpoT influences the expression of *arfB* by modulating the functions of ArfF and ArfG. Given the knowledge that (p)ppGpp, a metabolite of SpoT, regulates global transcription in bacteria through its connection with RNA polymerase,⁷ we assumed that the *spoT::Tn5* mutation epistatically interferes with transcription control of the arthrofactin biosynthesis genes.

To analyze the functional relationships among *arfB*, *arfF*, *arfG*, and *spoT*, we constructed expression plasmids carrying wild-type *arfF* (pArfF6032), *arfG* (pArfG6032), and *spoT* (pSoT6032) and introduced them into the *spoT::Tn5* mutant (Fig. 1C). The *spoT::Tn5* mutant carrying either pArfF6032 or pArfG6032 fully restored *arfB* expression to the wild-type MIS38 level. This indicates that both ArfF and ArfG can transactivate the arthrofactin synthetase gene and that they might act subordinately to SpoT regulation. Upon the introduction of pSpoT6032, neither regulatory (*arfF*, *arfG*) nor synthetase (*arfB*) gene expression was restored in the *spoT::Tn5* mutant. Failure

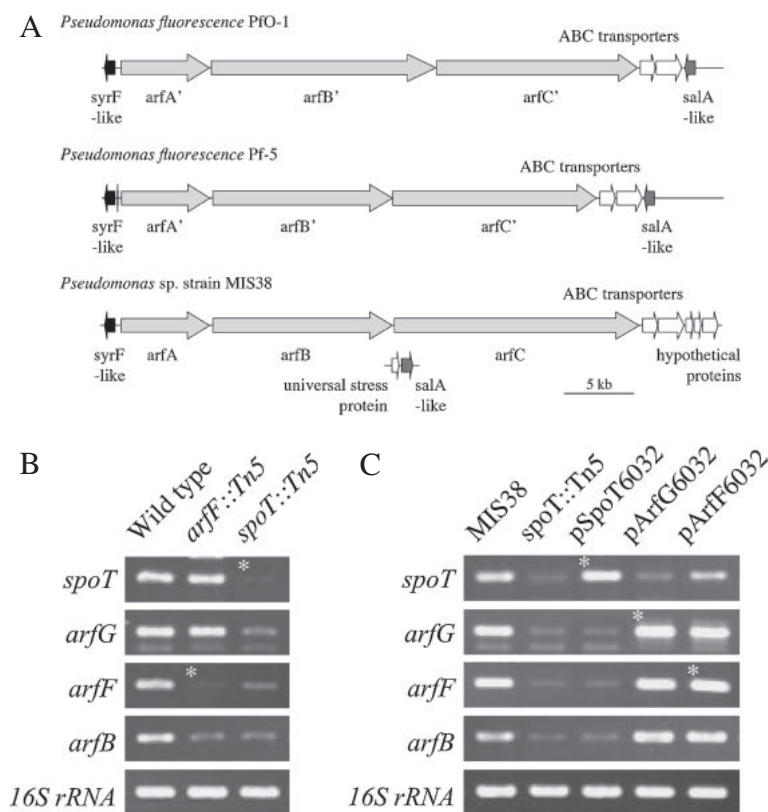


Fig. 1. Transcriptional Control of the Arthrofactin Biosynthesis Genes.

A, Organization of the genes responsible for the biosynthesis of arthrofactin-like lipopeptides among fluorescent *Pseudomonas*. Arrows indicate direction of transcription. Protein coding regions for the regulatory and synthetase genes are shaded. The bar indicates 5 kbp. B, RT-PCR analysis of the genes involved in arthrofactin production. RNA samples were prepared from 1-d cultures of the wild type, *spoT::Tn5*, and the *arfF::Tn5* mutant and subjected to RT-PCR analysis. Target genes are denoted at the left (*spoT*, *arfG*, *arfF*, *arfB*, and *16S rRNA*). C, Complementation analysis of the *spoT::Tn5* mutant. RNA samples were prepared from 1-d cultures of MIS38 (MIS38) and the *spoT::Tn5* mutant (*spoT::Tn5*) carrying empty pME6032, and MIS38 carrying pSpoT6032, pArfG6032, or pArfF6032, and were subjected to RT-PCR analysis. Manipulated genes are indicated by asterisks.

Table 2. *In Vivo* Gene Manipulation of *spoT* in MIS38 and Effects on Colony Formation Ability and the Level of Arthrofactin Production as Compared to Wild-Type MIS38 (100%)

Genotype	Schematic gene organization	Colony formation	Arthrofactin production
<i>spoT::Tn5</i>		slow	trace
<i>spoTnull</i>		not obtained	not determined
<i>spoTdelC</i>		normal	182.6 ± 8.7%

to complement the *spoT::Tn5* mutation with the wild-type *spoT* raises the possibility that Tn5 insertion changed the function of *spoT* or caused polar effects on adjacent genes.

In vivo gene manipulation of *spoT* in MIS38

The *spoT* gene of MIS38 contains an open reading frame (ORF) of 2,106 base pairs (bp) and encodes 701 amino acid (aa) residues. Nucleotide sequencing revealed that a single Tn5 insertion occurred in the

forward orientation 1,663 bp downstream from adenine of the first ATG codon (Table 2). To recapitulate the *spoT::Tn5* mutation, we introduced several different mutations in *spoT*. First we tried to remove *spoT* from the MIS38 genome by homologous recombination (*spoTnull*). The DNA fragments flanking *spoT* were amplified by PCR, cloned into suicide vector pCVD442-Km, and introduced into MIS38, but we failed to obtain a successful *spoT* null allele, probably due to the essential role of *spoT* in the normal growth of MIS38.

Because Tn5 insertion was identified near the 3' terminus of the *spoT* locus and the 5' region encoding the catalytic region of SpoT remained, we were concerned that the enzyme activity of SpoT should be modified, and successfully obtained the *spoT::Tn5* mutant, which is usually lethal in most Gram-negative bacteria.^{11,12} To examine this possibility, we cloned the 5' region of the *spoT::Tn5* locus in pCVD442-Km, introduced it into MIS38, and used it to replace the native *spoT* by homologous recombination. The resulting strain, *spoT_{delC}*, theoretically expressed the N-terminal segment of SpoT (M1 to E554) fused with a 24-residue segment derived from the Tn5 sequence. HPLC analysis indicated that the levels of arthrfactin production by the *spoT_{delC}* strain increased by about 1.8 fold as compared to the wild type, in sharp contrast to the *spoT::Tn5* mutant. Although this result conflicts with our expectations, *in vivo* gene manipulation of *spoT* indicates that the function of *spoT* is indeed connected with arthrfactin production.

Detection of the transcripts derived from the *spoT::Tn5* locus

A Pfam database search (<http://pfam.sanger.ac.uk/>) revealed that the predicted structure of MIS38 SpoT (701 aa) is composed of multiple domains, including the HDc superfamily (residues 45–144), the RelA/SpoT-like superfamily (235–345), and the TGS (389–448) and ACT (626–692) domains (Fig. 2A). In the *spoT::Tn5* mutant, the ORF of *spoT* was divided by Tn5 insertion, and probably encodes the N-terminal (SpoT_{Nter}) and C-terminal (SpoT_{Cter}) segments of SpoT. SpoT_{Nter} includes the HDc, RelA/SpoT, and TGS domains. SpoT_{Cter} contains only the ACT domain. To determine which *spoT* transcripts are generated in the *spoT::Tn5* mutant, we designed primer sets capable of amplifying distinct portions of the *spoT::Tn5* locus and analyzed the transcript species derived from *spoT* (Fig. 2B).

RT-PCR analysis of the *spoT* transcripts indicated that expression of the 5' region of *spoT* was retained in the *spoT::Tn5* mutant. Furthermore, the 3' region of *spoT* starting from Tn5 was weakly expressed in it, probably due to the promoter activity in kanamycin resistance gene cassette in Tn5. Nucleotide sequencing of the RT-PCR product verified that a small ORF (136 aa) was reconstructed in the 3' transcript, which possessed a potential ribosome binding site near a newly generated GTG start codon (Fig. 2C). This suggests that Tn5 insertion split the original ORF of *spoT* to encode distinct N-terminal (M1 to E554 plus 24 residues derived from *Tn5*) and C-terminal (M566 to A701) segments of MIS38 SpoT.

Expression of the distinct segments of SpoT in MIS38

To determine whether the N-terminal or C-terminal segment of SpoT influences the productivity of arthrfactin, expression plasmids carrying *spoT_{Nter}* (pSpoT6032_{Nter}) and *spoT_{Cter}* (pSpoT6032_{Cter}) were constructed to express SpoT_{Nter} and SpoT_{Cter} in wild-type MIS38 (Table 3). We also tested the pME6032 plasmid carrying *spoT_{Cter}* in the anti-sense orientation (pSpoT6032A_{Cter}) to verify the correct functioning of the small ORF in *spoT_{Cter}*. MIS38, carrying pSpoT6032_{Nter}, exhibited no obvious changes in arthro-

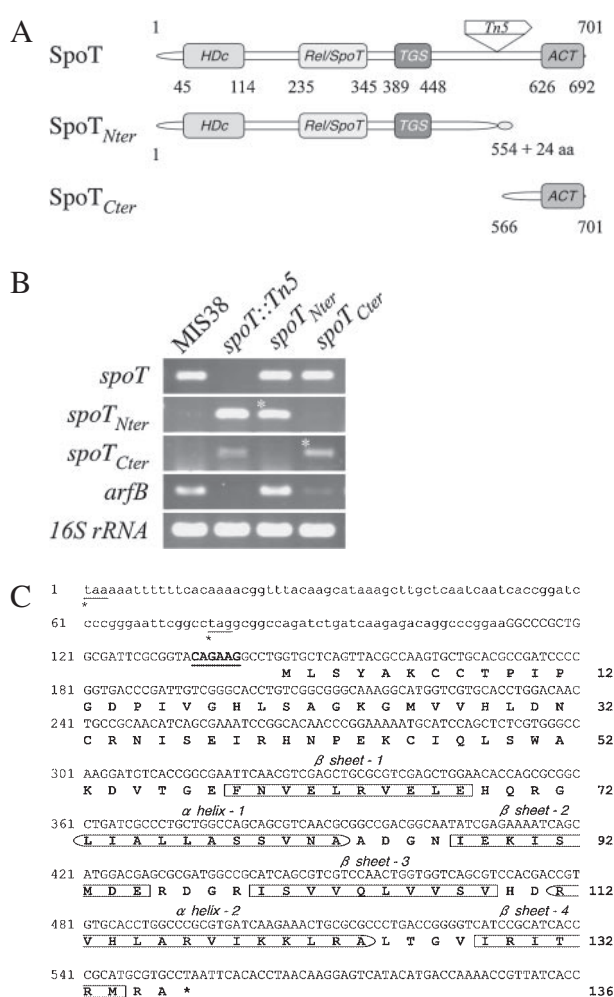
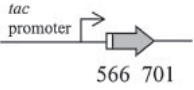
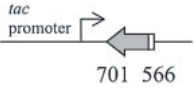


Fig. 2. The Distinct Transcripts of *spoT* Generated in the *spoT::Tn5* Mutant.

A, Predicted protein structure of MIS38 SpoT. Multiple domains in SpoT were predicted by a Pfam database search, and are denoted by the domain name with the amino acid position. The position of the Tn5 insertion in the *spoT::Tn5* mutant is indicated. B, RT-PCR analysis of *spoT::Tn5* transcripts. RNA samples were prepared from MIS38 (MIS38) and the *spoT::Tn5* mutant (*spoT::Tn5*) carrying empty pME6032, and MIS38 carrying pSpoT6032_{Nter} or pSpoT6032_{Cter} grown in LB medium at 30 °C for 1 d and subjected to RT-PCR using specific primer pairs spanning the Tn5 and *spoT* regions, as described in Table 1. Target genes are indicated at the left (*spoT*, *spoT_{Nter}*, *spoT_{Cter}*, *arfB*, and *16S rRNA*). Introduced genes are indicated by asterisks. C, Nucleotide sequence of the 3' portion of the *spoT::Tn5* locus and the predicted protein structure of SpoT_{Cter} (136 aa). Small and large letters indicate the nucleotide sequences of the Tn5 and MIS38 DNAs respectively. The stop codons upstream of the small ORF are underlined and indicated by asterisks. A potential ribosome binding site near the first GTG codon is underlined and in bold. The $\alpha\beta\alpha\beta$ fold of the ACT domain is boxed.

factin production. On the other hand, the introduction of pSpoT6032_{Cter} reduced the productivity of arthrfactin to about 6% of the level of MIS38 carrying empty pME6032. This negative effect was not observed for the pSpoT6032A_{Cter} construct. RT-PCR analysis indicated that the level of *arfB* expression counteracted *spoT_{Cter}* expression in each strain examined. The *arfB* transcript was barely detectable in MIS38 harboring pSpoT6032_{Cter} (Fig. 2B). The defect in arthrfactin production in the *spoT::Tn5* mutant might be due to the dominant-negative effect delivered by the artificial expression of SpoT_{Cter}.

Table 3. Expression of a Distinct Segment of SpoT in MIS38 and Effects on Colony Formation Ability and the Level of Arthrofactin Production as Compared to MIS38 Carrying Empty pME6032 (100%)

Plasmid	Schematic gene organization	Colony formation	Arthrofactin production
pSpoT6032 _{Nter}		normal	94.4 ± 1.9%
pSpoT6032 _{Cter}		slow	6.2 ± 0.7%
pSpoT6032A _{Cter}		normal	94.3 ± 5.2%

Physiological characterization of the transformed strains of MIS38

The phenotypes of MIS38 carrying pSpoT6032_{Nter} and pSpoT6032_{Cter} were compared with those of MIS38 and the *spoT::Tn5* mutant carrying empty pME6032 (Fig. 3). In LB liquid culture, MIS38 carrying pSpoT6032_{Cter} exhibited a retarded growth rate with diminished final cell densities, suggesting that the moderate growth arrest was caused by the expression of SpoT_{Cter} (Fig. 3A). In this experiment, we noticed that most of the MIS38 cells carrying pSpoT6032_{Cter} adhered to the surface of the glass flask and could not be dispersed despite vigorous shaking at 150 rpm. This indicates the high propensity to revert to the solid phase caused by the expression of SpoT_{Cter}.

Motility was examined by swarming on a 0.7% LB agar plate (Fig. 3B). MIS38 carrying empty pME6032 and pSpoT6032_{Nter} actively swarmed on the surface of the LB agar plate for 12 h; the swarmed areas were 11.3 cm² and 12.8 cm² respectively. Swarming was abolished in the *spoT::Tn5* mutant (swarmed area, 0.3 cm²) and MIS38 carrying pSpoT6032_{Cter} (0.6 cm²). Next, we tested the strains for biofilm formation on the surfaces of polypropylene tubes (Fig. 3C). MIS38 carrying empty pME6032, pSpoT6032_{Nter}, and pSpoT6032_{Cter} formed biofilms early in the incubation period (1 or 2 d), what then declined, probably due to detachment of the cells. MIS38 carrying pSpoT6032_{Cter} again formed thick biofilms following incubation for 4 or 5 d. The pattern of biofilm formation increase later in the cultivation period was also observed for the *spoT::Tn5* mutant. Growth conditions after prolonged incubation should evoke the *spoT::Tn5* mutant and MIS38 carrying pSpoT6032_{Cter} to form robust biofilms.

Biofilm cells were observed by SEM at 4 d after cultivation (Fig. 4). In cultures of MIS38 carrying empty pME6032 and pSpoT6032_{Nter}, a small number of rod-shaped cells were flatly attached to the surface of tube. The three-dimensional structures of the biofilm cells were observed for both the *spoT::Tn5* mutant and MIS38 carrying pSpoT6032_{Cter}. The bacterial cells of the *spoT::Tn5* mutant were more spherical and shorter along the major axis than those of the wild type, indicating disruption of MIS38 cell division. The MIS38 cells carrying pSpoT6032_{Cter} were rather filamentous and grew into dense aggregates connected by fibril matrices. SEM observation revealed that the cell proper-

ties of the *spoT::Tn5* mutant and MIS38 carrying pSpoT6032_{Cter} were not identical, but resulted in similar sessile morphotypes.

Production of ppGpp in the transformed strains of MIS38

We monitored the cellular levels of ppGpp by HPLC analysis (Fig. 5). At 2 d, ppGpp was not detected in MIS38 carrying empty pME6032 and pSpoT6032_{Nter}, but ppGpp levels were high in the *spoT::Tn5* mutant and MIS38 carrying pSpoT6032_{Cter} (53 min peak). Two additional peaks appeared in these two strains (36 and 43 min). It has been reported that formic acid extraction is useful for the rapid isolation of nucleotides, but results in undesired degradation of ppGpp into other guanosine nucleotides.²²⁾ Taken together, these data indicate that stand-alone expression of SpoT_{Cter} increases the ppGpp pool similarly to the *spoT::Tn5* mutation.

Discussion

In *E. coli* and related Gram-negative bacteria, RelA and SpoT are responsible for the accumulation of (p)ppGpp.¹⁰⁾ RelA is a ribosome-associated protein, and mainly senses amino acid starvation. SpoT is a putative cytosolic protein that synthesizes pppGpp in response to other nutritional forms of depletion. The two proteins are homologous, but RelA is not capable of degrading ppGpp. Dissection of *E. coli* RelA described the feature of the C-terminal domain that senses amino acid starvation, possibly *via* interaction with the ribosome.^{23,24)} The dualfunction of SpoT, possessing both ppGpp hydrolase and pppGpp synthetase activities, is similar to those of the RSH proteins in most Gram-positive bacteria. The crystal structure of Rel_{Seq} from *Streptococcus equisimilis* suggests a model for the catalysis of RSH, in which a hinge-like movement of the C-terminal region alternatively blocks the separate active sites in the N-terminal region responsible for the hydrolysis and synthesis of (p)ppGpp.²⁵⁾ This evidence reveals that the catalysis of RelA, SpoT, and RSH is differently regulated by the C-terminal regulatory region.

Previous analysis has indicated that deletion of the C-terminal region from RSH has various effects on enzyme activity.¹³⁾ For example, C-terminal deletion of Rel_{Seq} results in ribosome-independent production of

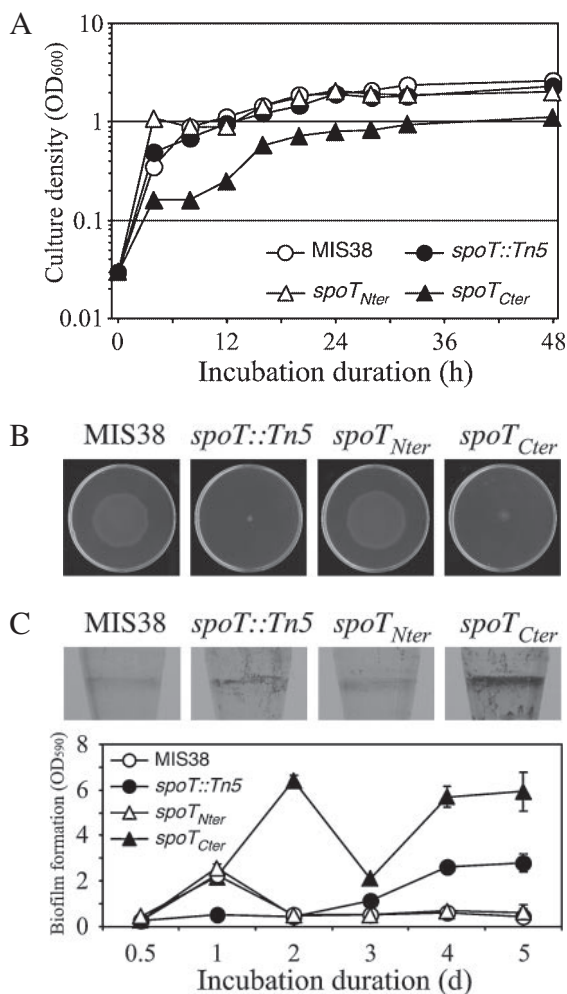


Fig. 3. Physiological Characterization of Transformed Strains of MIS38.

A, Growth curve in LB liquid culture. The optical densities (OD₆₀₀) of MIS38 (hollow circles) and the *spoT::Tn5* mutant (solid circles) carrying empty pME6032, and MIS38 carrying pSpoT6032_{Nter} (hollow triangles) or pSpoT6032_{Cter} (solid triangles) were determined in LB liquid culture at 30 °C. The experiment was repeated 3 times, and average values are shown. B, Swarming on a 0.7% agar LB plate. Swarming patterns were compared among MIS38 (MIS38) and the *spoT::Tn5* (*spoT::Tn5*) mutant carrying empty pME6032, and MIS38 carrying pSpoT6032_{Nter} (*spoT_{Nter}*) or pSpoT6032_{Cter} (*spoT_{Cter}*). C, Biofilm formation on the surface of polypropylene tube. After cultivation for 4 d at 20 °C, the area of the biofilm ring was stained with 0.1% w/v crystal violet (CV) solution and observed by light microscope. CV staining was conducted at different times (0.5, 1, 2, 3, 4, and 5 d), and then the CV adhering to the biofilm was dissolved in 95% ethanol, the absorbance of which at 590 nm was measured. All data sets reflect averages of triplicate experiments. Error bars indicate the standard error of the mean.

(p)ppGpp and increases pppGpp synthesis.²⁶⁾ Deleting the C-terminal region of Rel_{mtb} from *Mycobacterium tuberculosis* makes it non-responsive to the ribosome, but in this case the enzyme activity does not change.²⁷⁾ Our present study indicates that C-terminal truncation of MIS38 SpoT increases the level of arthrofactin production (*spoT_{delC}*) (Table 2). It is unclear how the enzyme activity of MIS38 SpoT is changed by C-terminal deletion, since the ppGpp levels of the wild type MIS38 and the *spoT_{delC}* strain are below the detectable range (data not shown). Given that arthrofactin production is abrogated in the *spoT::Tn5* mutant in coordination with a moderate accumulation of ppGpp, we assume that ppGpp has a negative effect on arthrofactin production.

Our C-terminal deletion of MIS38 SpoT should decrease pppGpp synthesis or induce ppGpp hydrolysis, so that arthrofactin production might be derepressed by lowering the (p)ppGpp levels.

The regulation of SpoT activity is still elusive. It has been proposed that interaction between the TGS region of SpoT and the acyl carrier protein (ACP) ensures conformational changes in SpoT and alters the balance of hydrolytic and synthetic activities in *E. coli*.²⁸⁾ Interaction between SpoT and the conserved bacterial G protein CgtA, which is involved in the global stress response in *Vibrio cholerae*, has also been documented.²⁹⁾ These reports suggest that SpoT activity is maintained by physical interaction with metabolic regulators.¹⁰⁾ The C-terminal region of MIS38 SpoT, examined in this study, does not contain the TGS domain, but includes the ACT domain (Fig. 2C). The ACT domain is a structural domain common to aspartate kinase, chorismate mutase, and TyrA (prephenate dehydrogenase), and generally consists of 70–80 residues with two α helices and four β strands (a $\beta\alpha\beta\beta\alpha\beta$ fold).³⁰⁾ The ACT domain was initially identified among enzymes for amino acid and purine synthesis. Extensive analysis indicated broader distribution of ACT and ACT-like domains in many enzymes and transcription factors.³¹⁾

The ACT domain has been found to bind small ligands such as amino acids multilaterally, which facilitates contact with partner proteins and transmits conformational changes within allosteric enzymes.^{32,33)} Little is known about the regulatory ligands or cellular components that are recognized by the ACT domain of SpoT.³¹⁾ Our study indicated that forced expression of SpoT_{Cter} increased the ppGpp level in the *relA*⁺ background of MIS38 (Fig. 5). Since the ACT domain does not have catalytic activity, indirect effects might account for the accumulation of ppGpp. One possibility is interference with exogenous SpoT. In a study of *M. tuberculosis*, a role in oligomerization has been suggested for the C-terminal region of Rel_{mtb}.²⁷⁾ If SpoT_{Cter} can be folded into a stable domain structure in MIS38 and can modulate the enzyme assembly of SpoT, the balance of the synthesis and hydrolysis of (p)ppGpp is influenced.

Another possibility is suggested by artificial stress. If the binding-ligand of the ACT domain in SpoT is involved in the main control of the stringent response and what are absorbed by a large amount of SpoT_{Cter}, it is hypothesized that MIS38 can not monitor the nutrient state property and aberrantly accumulates (p)ppGpp through catalysis of RelA or SpoT. This is supported by the fact that not only the *E. coli* BL21 (*relA*⁺/*spoT*⁺) but also the *E. coli* CF8295 (*relA*⁻/*spoT*⁻) strain showed growth arrest even in LB nutrient medium due to stable expression of a similar C-terminal region of *E. coli* SpoT.³⁴⁾ This indicates that the target of the ACT domain of SpoT is distinct from RelA and SpoT. The native function of the ACT domain in MIS38 SpoT must be identified by the *relA/spoT* mutants with the reference to *E. coli* SpoT.

Manipulation of *spoT* significantly influenced biofilm formation in MIS38 (Fig. 3C). It is noteworthy that MIS38 showed a single peak of biofilm formation at 1 d and that this peak disappeared in the *spoT::Tn5* mutant. This suggests that intact SpoT is important to the short-

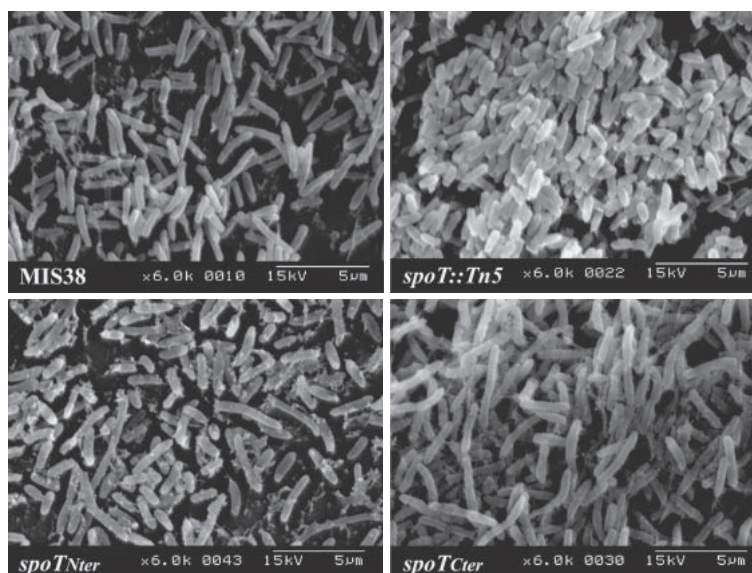


Fig. 4. SEM Observations of Biofilm Cells.

Biofilms of MIS38 (MIS38) and the *spoT::Tn5* mutant (*spoT::Tn5*) carrying empty pME6032, and of MIS38 carrying pSpoT6032_{Nter} (*spoT_{Nter}*) or pSpoT6032_{Cter} (*spoT_{Cter}*) were developed in LB medium kept standing at 20 °C for 4 d.

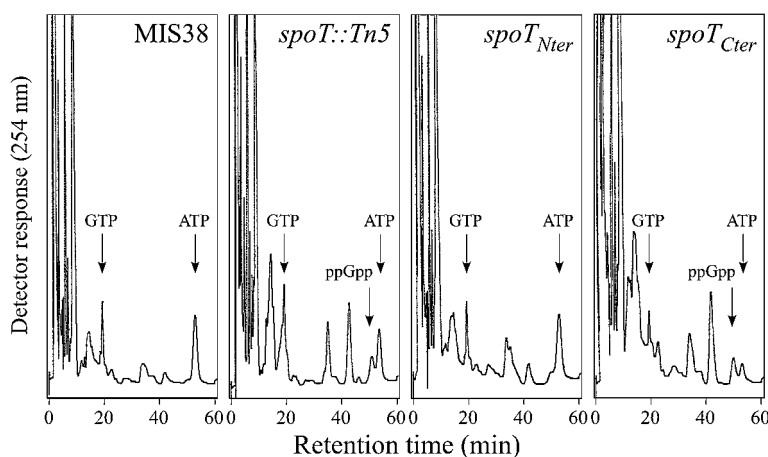


Fig. 5. Accumulation of ppGpp in MIS38 and the *spoT::Tn5* Mutant Carrying Empty pME6032, and of MIS38 Carrying pSpoT6032_{Nter} (*spoT_{Nter}*) or pSpoT6032_{Cter} (*spoT_{Cter}*).

The intracellular levels of ppGpp were monitored by ion-pair reverse-phase HPLC. Eluted nucleotides were monitored by sample absorbance at 254 nm. The positions of standards (GTP, ppGpp, and ATP) are indicated by arrows. ppGpp was eluted at 53 min under our assay conditions.

term response of MIS38 in establishing surface attachment. The *spoT::Tn5* mutant and MIS38 carrying pSpoT6032_{Cter} formed extensive biofilms at the later stage of cultivation (Fig. 3C). Since both strains accumulate higher levels of ppGpp, probably due to the expression of SpoT_{Cter} (Fig. 5), MIS38 should overestimate starvation stress and transit to a more tolerant state. In a recent study of *E. coli*, SpoT-mediated reduction of ppGpp levels triggered biofilm induction on ribosomal stress.³⁵ This inconsistency might have been due to the different demands and efficacy of (p)ppGpp signaling among the species.

In addition, MIS38, carrying pSpoT6032_{Cter}, formed more biofilm than the *spoT::Tn5* mutant (Fig. 3C). We expressed *spoT_{Cter}* constitutively with the strong *tac* promoter in MIS38, and the expression levels of *spoT_{Cter}* appeared to be higher in MIS38 carrying pSpoT6032_{Cter} rather than the *spoT::Tn5* mutant (Fig. 2B). This might have caused increases in basal ppGpp levels and

resulting in a severe phenotype. This is in agreement with the fact that the stringent response is controlled by cellular (p)ppGpp pools in a dose-dependent manner.³⁶

The stringent response is important not only for the ecological fitness of bacteria. It also governs the production of various useful bioactive products.³⁶ In *Streptomyces clavuligerus*, the production of two antibiotics, cephamycin C and clavulanic acid, is positively or negatively regulated by a Gram-positive homolog of SpoT.^{37,38} Global microarray analysis using *E. coli* *relA/spoT* mutants indicated that the stringent response includes the control of virtually all macromolecular synthesis and intermediary metabolism.⁸ Arthrofactin is an excellent surface-activating agent that exhibits weak antifungal activities.^{3,4} The present study indicates that arthrofactin production is closely linked with the function of SpoT (Table 2). Because SpoT is the main regulator of the stringent response, we believe that

arthrofactin plays multiple roles in the physiological adaptation of MIS38 in nature, including antibiotics, avoidance of unfavorable conditions, and the metabolism of hydrocarbons. Further investigation of SpoT function may lead to higher yields of the objective secondary metabolites.

Acknowledgments

E. coli SM10 λ -pir and pCVD442 were kindly supplied by Dr. D. A. Hogan (Dartmouth Medical School) and Dr. R. Kolter (Harvard Medical School). This study was supported by a Grant-in-Aid for Scientific Research from the Japan Society for the Promotion of Science (JSPS, to KW).

References

- Schwarzer D, Finking R, and Marahiel MA, *Nat. Prod. Rep.*, **20**, 275–287 (2003).
- Morikawa M, Daido H, Takao T, Murata S, Shimonishi Y, and Imanaka T, *J. Bacteriol.*, **175**, 6459–6466 (1993).
- Morikawa M, Hirata Y, and Imanaka T, *Biochim. Biophys. Acta*, **1488**, 211–218 (2000).
- Roongsawang N, Hase K, Haruki M, Imanaka T, Morikawa M, and Kanaya S, *Chem. Biol.*, **10**, 869–880 (2003).
- Roongsawang N, Washio K, and Morikawa M, *ChemBiochem*, **8**, 501–512 (2007).
- Washio K, Lim SP, Roongsawang N, and Morikawa M, *Biosci. Biotechnol. Biochem.*, **74**, 992–999 (2010).
- Magnusson LU, Farewell A, and Nyström T, *Trends Microbiol.*, **13**, 236–242 (2005).
- Traxler MF, Summers SM, Nguyen HT, Zacharia VM, Hightower GA, Smith JT, and Conway T, *Mol. Microbiol.*, **68**, 1128–1148 (2008).
- Braeken K, Moris M, Daniels R, Vanderleyden J, and Michiels J, *Trends Microbiol.*, **14**, 45–54 (2006).
- Battesti A and Bouveret E, *J. Bacteriol.*, **191**, 616–624 (2009).
- Xiao H, Kalman M, Ikehara K, Zemel S, Glaser G, and Cashel M, *J. Biol. Chem.*, **266**, 5980–5990 (1991).
- Murray KD and Bremer H, *J. Mol. Biol.*, **259**, 41–57 (1996).
- Potrykus K and Cashel M, *Annu. Rev. Microbiol.*, **62**, 35–51 (2008).
- Heeb S, Itoh Y, Nishijyo T, Schnider U, Keel C, Wade J, Walsh U, O’Gara F, and Haas D, *Mol. Plant Microbe Interact.*, **13**, 232–237 (2000).
- Takei D, Washio K, and Morikawa M, *Biotechnol. Lett.*, **30**, 1447–1452 (2008).
- Donnenberg MS and Kaper JB, *Infect. Immun.*, **59**, 4310–4317 (1991).
- Iijima S, Washio K, Okahara R, and Morikawa M, *Microb. Biotechnol.*, **2**, 361–369 (2009).
- Funabashi H, Mie M, Yanagida Y, Kobatake E, and Aizawa M, *Biotechnol. Lett.*, **24**, 269–273 (2002).
- de Bruijn I and Raaijmakers JM, *Appl. Environ. Microbiol.*, **75**, 4753–4761 (2009).
- Wang N, Lu SE, Records AR, and Gross DC, *J. Bacteriol.*, **188**, 3290–3298 (2006).
- Lim SP, Roongsawang N, Washio K, and Morikawa M, *J. Appl. Microbiol.*, **107**, 157–166 (2009).
- Lagosky PA and Chang FN, *Biochem. Biophys. Res. Commun.*, **84**, 1016–1024 (1978).
- Schreiber G, Metzger S, Aizenman E, Roza S, Cashel M, and Glaser G, *J. Biol. Chem.*, **266**, 3760–3767 (1991).
- Gropp M, Strausz Y, Gross M, and Glaser G, *J. Bacteriol.*, **183**, 570–579 (2001).
- Hogg T, Mechold U, Malke H, Cashel M, and Hilgenfeld R, *Cell*, **117**, 57–68 (2004).
- Mechold U, Murphy H, Brown L, and Cashel M, *J. Bacteriol.*, **184**, 2878–2888 (2002).
- Avarbock A, Avarbock D, Teh JS, Buckstein M, Wang ZM, and Rubin H, *Biochemistry*, **44**, 9913–9923 (2005).
- Battesti A and Bouveret E, *Mol. Microbiol.*, **62**, 1048–1063 (2006).
- Raskin DM, Judson N, and Mekalanos JJ, *Proc. Natl. Acad. Sci. USA*, **104**, 4636–4641 (2007).
- Ettema TJ, Brinkman AB, Tani TH, Rafferty JB, and van der Oost J, *J. Biol. Chem.*, **277**, 37464–37468 (2002).
- Chipman DM and Shaanan B, *Curr. Opin. Struct. Biol.*, **11**, 694–700 (2001).
- Liberles JS, Thóroflsson M, and Martínez A, *Amino Acids*, **28**, 1–12 (2005).
- Grant GA, *J. Biol. Chem.*, **281**, 33825–33829 (2006).
- Fujita C, Nishimura A, Iwamoto R, and Ikehara K, *Biosci. Biotechnol. Biochem.*, **66**, 1515–1523 (2002).
- Boehm A, Steiner S, Zaehring F, Casanova A, Hamburger F, Ritz D, Keck W, Ackermann M, Schirmer T, and Jenal U, *Mol. Microbiol.*, **72**, 1500–1516 (2009).
- Jain V, Kumar M, and Chatterji D, *J. Microbiol.*, **44**, 1–10 (2006).
- Jin W, Ryu YG, Kang SG, Kim SK, Saito N, Ochi K, Lee SH, and Lee KJ, *Microbiology*, **150**, 1485–1493 (2004).
- Gomez-Escribano JP, Martín JF, Hesketh A, Bibb MJ, and Liras P, *Microbiology*, **154**, 744–755 (2008).